Immunity, Vol. 20, 393–406, April, 2004, Copyright ©2004 by Cell Press

Rolling Adhesion through an Extended Conformation of Integrin $\alpha_L\beta_2$ and Relation to α I and β I-like Domain Interaction

Azucena Salas,[1] Motomu Shimaoka,[2] Avi N. Kogan,[3] Charlotte Harwood,[1] Ulrich H. von Andrian,[1] and Timothy A. Springer[1,*]
The CBR Institute for Biomedical Research
[1]Department of Pathology
[2]Department of Anesthesia
[3]Program in Biophysics
Harvard Medical School
200 Longwood Avenue
Boston, Massachusetts 02115

Summary

In vivo, β_2 integrins and particularly $\alpha_L\beta_2$ (LFA-1) robustly support firm adhesion of leukocytes, but can also cooperate with other molecules in supporting rolling adhesion. Strikingly, a small molecule α/β I-like allosteric antagonist, XVA143, inhibits LFA-1-dependent firm adhesion, while at the same time it enhances adhesion in shear flow and rolling both in vitro and in vivo. XVA143 appears to induce the extended conformation of integrins as shown by increased activation epitope exposure. Fab to the β_2 I-like domain converts firm adhesion to rolling adhesion, but does not enhance adhesion. Residue α_L-Glu-310 in the linker following the I domain is critical for communication to the β_2 I-like domain, rolling, integrin extension, and activation by Mn^{2+} of firm adhesion. The results demonstrate the importance of integrin extension in rolling, and suggest that rolling and firm adhesion are mediated by extended conformations of $\alpha_L\beta_2$ that differ in the affinity of the α_L I domain for ICAM-1.

Introduction

Integrins are a family of heterodimeric receptors that use bidirectional (inside-out and outside-in) signaling to integrate the intracellular and extracellular environments. Some integrins contain an inserted (I) domain in their α subunits, including LFA-1 (integrin $\alpha_L\beta_2$) (Humphries, 2000; Shimaoka et al., 2002). LFA-1 binds IgSF cell surface molecules known as intercellular adhesion molecules (ICAMs) and functions in lymphocyte recognition of other cells and in leukocyte trafficking between blood, tissue, and lymph (Springer, 1994). The ligand binding site of LFA-1 is wholly contained within the α_L I domain (Lu et al., 2001b; Shimaoka et al., 2001, 2003b). One- and two-turn axial displacements in the C-terminal direction of the α_L I domain α7-helix are linked to rearrangements around the ligand binding site at the metal ion dependent adhesion site (MIDAS) and to increases in affinity for ICAM-1 of up to 10,000-fold (Huth et al., 2000; Shimaoka et al., 2003b). The I-like domain in the integrin β_2 subunit undergoes conformational changes during activation that allosterically regulate binding through the α_L I domain (Lu et al., 2001c; Yang et al., 2004a, 2004b). Like the α_L I domain, the β_2 I-like domain contains a MIDAS that plays a key role in its function.

Although there are no overall structures for integrins that contain I domains, rapid progress has recently been made in understanding the structural basis for regulation of ligand binding in integrins that lack I domains. In these integrins, the β subunit I-like domain and the α-subunit β-propeller domain constitute the ligand binding site (Takagi et al., 2003; Xiong et al., 2002; Yahalom et al., 2002). A crystal structure for most of the extracellular domains of integrin $\alpha_V\beta_3$ revealed an unexpected overall V-shaped organization, in which the ligand binding domains in the headpiece are bent toward the cell membrane by extensive interactions with tailpiece domains (Takagi et al., 2002; Xiong et al., 2001). The extreme bend in the α and β subunits occurs at a location termed the "genu." Based on evidence from the NMR structure of β_2 subunit I-EGF domains (Beglova et al., 2002), together with mapping of activation-dependent or activation-inducing mAbs and sites of interaction with α that constrain β_2 integrins in the resting conformation (Lu et al., 2001a; Zang and Springer, 2001), the bent conformation was proposed to represent a low-affinity state of the integrin, and a switchblade-like opening was proposed to occur upon activation. Indeed, EM and mutational studies of integrins $\alpha_V\beta_3$ and $\alpha_5\beta_1$ have directly demonstrated at least three distinct conformational states (Takagi et al., 2002, 2003). These correspond to the bent conformation seen in the crystal structure that has low affinity for ligand (Figure 1F), and two extended conformations that differ in the angle between the β I-like and hybrid domains (Figures 1G and 1H). The extended conformations with the open (Figure 1H) and closed (Figure 1G) headpieces appear to have high and intermediate affinity for ligand, respectively. Recent mutagenesis, epitope mapping, and solution X-ray scattering studies have supported integrin extension and hybrid domain swing-out in the open headpiece conformation (Luo et al., 2003b; Mould et al., 2003a, 2003b) while ruling out an alternative model of headpiece separation (Luo et al., 2003a; Mould et al., 2003b).

The integrin $\alpha_L\beta_2$ appears to undergo similar conformational transitions, as shown with epitopes that become exposed upon LFA-1 activation and map to β_2 I-EGF domains 2 and 3 (Beglova et al., 2002) (Figures 1A–1E). Work with a class of small molecules termed α/β I-like allosteric antagonists also suggests analogous conformational changes in $\alpha_L\beta_2$. These compounds bind to the MIDAS of the β_2 I-like domain, and also to the α_L-subunit (Shimaoka et al., 2003a). They structurally resemble small molecule RGD-based antagonists in containing an absolutely required carboxyl group that is thought to bind to the β_2 I-like domain MIDAS. The α/β I-like allosteric antagonists, like RGD-based α/β I-like competitive antagonists, also appear to bind across the interface between the α-subunit β-propeller and β-subunit I-like domains (Shimaoka et al., 2003a). Furthermore, both classes of compounds induce the extended integrin conformation, as shown by exposure of activation epitopes (Kouns et al., 1992; Shimaoka et al., 2003a;

*Correspondence: springeroffice@cbr.med.harvard.edu

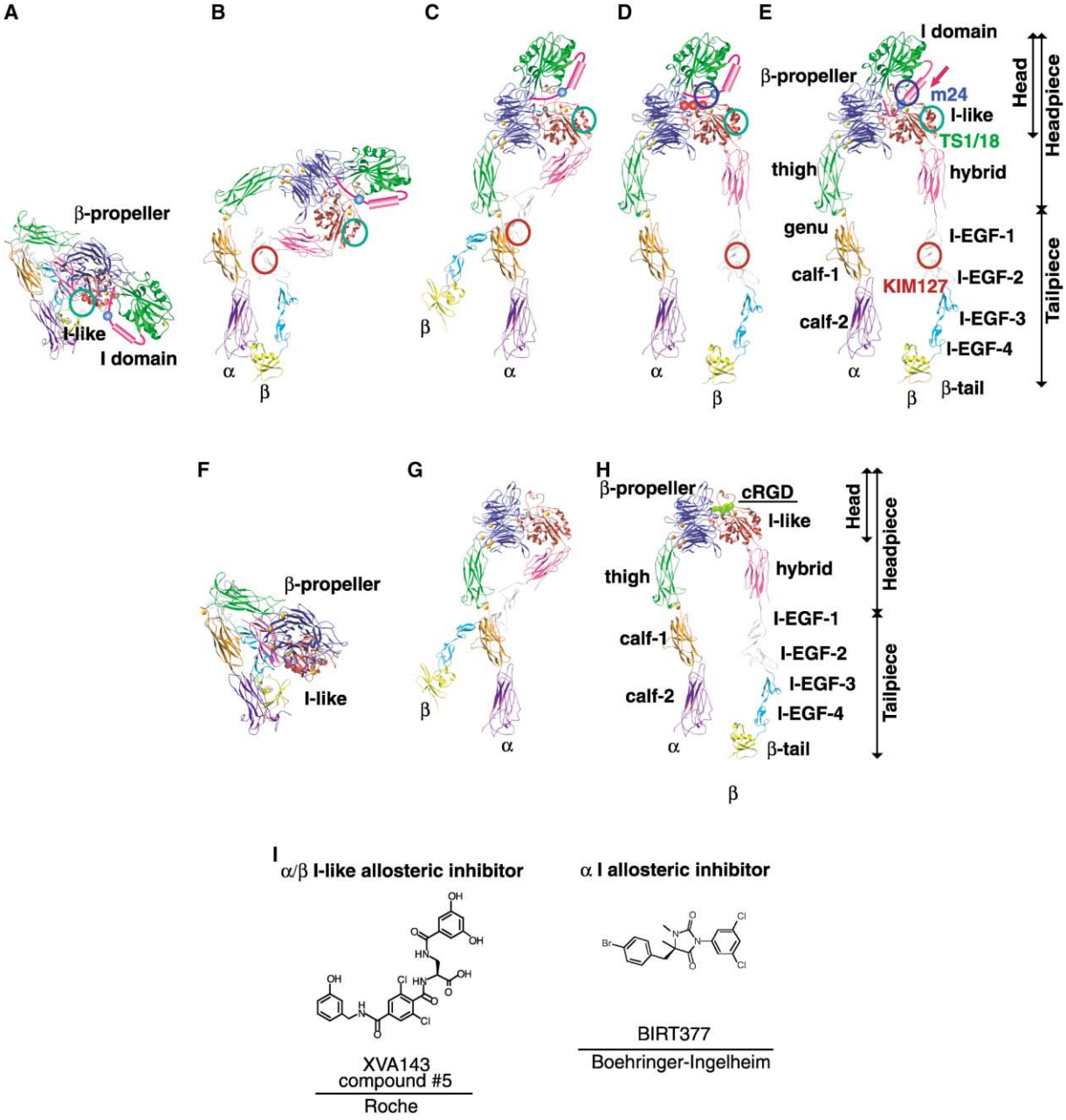

Figure 1. Conformational States for Integrins and Structure of $\alpha_L\beta_2$ Antagonists

(A–E) Model for $\alpha_L\beta_2$ integrin activation. The models for all of the extracellular domains except for the I domain (Springer, 2002) are based on conformational states of $\alpha_V\beta_3$ defined by negative stain electron microscopy (Takagi et al., 2002), crystallography (Xiong et al., 2002), NMR (Beglova et al., 2002), and mapping of activation epitopes (Lu et al., 2001a, 2001c). The α_L I domain is a cartoon based on crystal structures (Shimaoka et al., 2003b). The I domain is joined at the point of its insertion in the β-propeller domain but its orientation is arbitrary; the I domain is shown at slightly larger scale for emphasis. The C-terminal I domain α-helix is represented by a red cylinder, and α_L Glu-310 in the linker as a blue sphere. The positions of the epitope recognized by the TS1/18 Fab used here, and activation epitopes, are circled. Epitopes are circled only in the conformations in which they are thought to be exposed. (A) Bent conformation with low affinity. (B and C) LFA-1 with a closed headpiece and closed I domain in partially (B) or fully (C) extended states. (D) Extended conformation with open headpiece, and closed I domain, in the presence of XVA143, represented by three red spheres. (E) Extended conformation with open headpiece and open I domain.

(F–H) Model for $\alpha_V\beta_3$ integrin activation, with at least three conformations of the extracellular domain (Takagi et al., 2002). (F) Bent, low-affinity conformation. (G) Extended conformation with closed headpiece. (H) Extended conformation with open headpiece. (I) Chemical structures of small molecule $\alpha_L\beta_2$ antagonists used in this study.

Takagi et al., 2002), and for $\alpha_V\beta_3$, by direct electron microscopic observation (Takagi et al., 2002). By contrast, α I allosteric antagonists of $\alpha_L\beta_2$, which bind under the α7-helix of the α_L I domain and stabilize it in the closed conformation (Kallen et al., 1999; Lu et al., 2001b; Weitz-Schmidt et al., 2001), stabilize the bent conformation,

as shown by suppression of epitope induction by Mn^{2+} (Shimaoka et al., 2003a; Woska et al., 2001).

$\alpha_L\beta_2$ and the other β_2 integrins are far more facile in supporting firm adhesion than rolling adhesion. In many in vitro and in vivo systems in which β_2 integrins mediate firm adhesion and selectins mediate tethering and rolling adhesion, β_2 integrins are not seen to mediate tethering in shear flow or rolling (Lawrence and Springer, 1991; von Andrian et al., 1991). The α_4 integrins have been known for some time to mediate rolling as well as firm adhesion (Alon et al., 1995; Berlin et al., 1995), although they do not support rolling as efficiently as selectins (de Chateau et al., 2001). Nonetheless, in vivo studies have suggested for some time that while β_2 integrins cannot on their own mediate rolling, they can contribute to rolling together with selectins or α_4 integrins. Thus, when β_2 integrin function is blocked in vivo, and particularly when β_2 integrins or $\alpha_L\beta_2$ are blocked or eliminated together with one or more selectins or α_4 integrins, they can be seen to contribute to the accumulation of rolling cells, the stability of rolling, and the velocity of rolling cells in inflamed tissues (Forlow and Ley, 2001; Forlow et al., 2000; Henderson et al., 2001; Jung et al., 1998; Perry and Granger, 1991). By contrast, LFA-1 has been shown not to contribute to lymphocyte rolling in the high endothelial venules (HEV) of noninflamed lymph nodes (Warnock et al., 1998). In vitro, LFA-1 can mediate tethering in flow of leukocytes to ICAM-2 on platelets in the absence of selectin-mediated interactions (Weber and Springer, 1997). Moreover, special attention to the way in which ICAM-1 is coupled to the substrate, and to the type of LFA-1 bearing cell that is used, enables rolling solely through $\alpha_L\beta_2$ heterodimers to be detected in vitro (Salas et al., 2002; Sigal et al., 2000). Surprisingly, the wild-type α_L I domain expressed in isolation from other integrin domains by fusing its C terminus to an artificial membrane anchor supports rolling on ICAM-1 much more efficiently than $\alpha_L\beta_2$ heterodimers (Knorr and Dustin, 1997; Salas et al., 2002). Is an isolated, α_L I domain expressed on the cell surface in a better orientation to mediate tethering and rolling on ICAM-1 than a bent $\alpha_L\beta_2$ heterodimer? Isolated I domains locked in the open conformation with a disulfide-bond mediate firm adhesion (Salas et al., 2002), as do $\alpha_L\beta_2$ integrins activated by Mn^{2+}, activating antibodies, or physiologic activating stimuli (Campbell et al., 1998; Lawrence et al., 1995; Lawrence and Springer, 1991; Salas et al., 2002; Sigal et al., 2000; von Andrian et al., 1991). However, the ability of $\alpha_L\beta_2$ and other β_2 integrins to support rolling in vivo raises the intriguing possibility that rolling might be mediated by an intermediate conformation of $\alpha_L\beta_2$, with an extended conformation but with the I domain in a low or intermediate affinity state, corresponding approximately to the conformation depicted in Figures 1B and 1C.

How the overall conformation of $\alpha_L\beta_2$ relates to its ability to support rolling adhesion remains to be elucidated. The greater height above the cell surface of the headpiece in the extended conformation, and its altered orientation, appear more favorable for ligand encounter. Although both $\alpha_L\beta_2$ and α_4 integrins can mediate rolling, nothing is currently known about the global conformation of these integrins during rolling, or how overall conformation influences rolling. Here, we demonstrate the importance of integrin extension or conformational breathing in regulating rolling, and the interrelationship in $\alpha_L\beta_2$ between global conformation and the conformation of the α_L I domain, the β_2 I-like domain, and the coupling between these domains. We not only demonstrate the importance of integrin extension in rolling, but also make the surprising observation that α/β I-like allosteric antagonists markedly enhance or induce rolling adhesion while inhibiting firm adhesion.

Results

An α/β I-like Allosteric Antagonist Blocks Activation-Dependent Adhesion and in Contrast Enhances Rolling Adhesion on ICAM-1

In conditions in which $\alpha_L\beta_2$ is in a low-affinity conformation, such as in Ca^{2+}/Mg^{2+}, binding to soluble ICAM-1, even as a multimeric complex of ICAM-1-Fcα with FITC-anti-IgA, is weak (Figure 2A). Activation, for example by Mg^{2+}/EGTA or Mn^{2+}, is required to convert $\alpha_L\beta_2$ to a form that can bind soluble, multimeric ICAM-1 with high affinity (Figure 2A). However, appropriate conditions can be found where $\alpha_L\beta_2$ transfectants in Ca^{2+}/Mg^{2+} bind to ICAM-1 substrates in shear flow at 0.3–0.4 dyn/cm^2 (Figure 2B) as previously described (Salas et al., 2002; Sigal et al., 2000). Once cells are bound, their interactions with ICAM-1 substrates in Ca^{2+}/Mg^{2+} are relatively shear resistant, with cells continuing to roll or adhere at shear stresses ranging from 1 to 8 dyn/cm^2 (Figure 2B; Salas et al., 2002). The fraction of cells that roll increases markedly with increasing shear (Figure 2B). In contrast, in the presence of Mg^{2+}/EGTA (Figure 2E) or Mn^{2+} (data not shown), most cells adhere firmly to the ICAM-1 substrate and remain attached even after shear is increased to 16 dyn/cm^2.

Two classes of small molecule antagonists were used to probe the effect of the overall conformation of $\alpha_L\beta_2$ on its ability to mediate rolling. α I allosteric antagonists, represented here by BIRT377 (Figure 1I), bind in a hydrophobic pocket under the C-terminal α-helix of the I domain, stabilize the I domain in the closed, low-affinity conformation (Kallen et al., 1999; Last-Barney et al., 2001; Liu et al., 2001; Weitz-Schmidt et al., 2001), and also inhibit activation epitope exposure in $\alpha_L\beta_2$ (Shimaoka et al., 2003b; Woska et al., 2001), i.e., stabilize the bent conformation (Figure 1A). α/β I-like allosteric antagonists, represented here by XVA143 (Figure 1I), bind to the MIDAS of the β_2 I-like domain, as well as to a region of the α_L subunit that does not include the I domain (Shimaoka et al., 2003a; Welzenbach et al., 2002). α/β I-like allosteric antagonists were identified by their ability to inhibit high-affinity binding of $\alpha_L\beta_2$ to ICAM-1 (Fotouhi et al., 1999; Gadek et al., 2002), as subsequently confirmed (Shimaoka et al., 2003a; Welzenbach et al., 2002). α/β I-like allosteric antagonists bind to a critical interface for relaying conformational signals within $\alpha_L\beta_2$ (Shimaoka et al., 2003a). By binding to the β_2 I-like domain MIDAS, they stabilize the I-like domain in the active conformation and induce the extended conformation of $\alpha_L\beta_2$ as shown by exposure of activation epitopes, while blocking activation of the α_L I domain by the β_2 I-like domain (Figure 1D) (Shimaoka et al., 2003a).

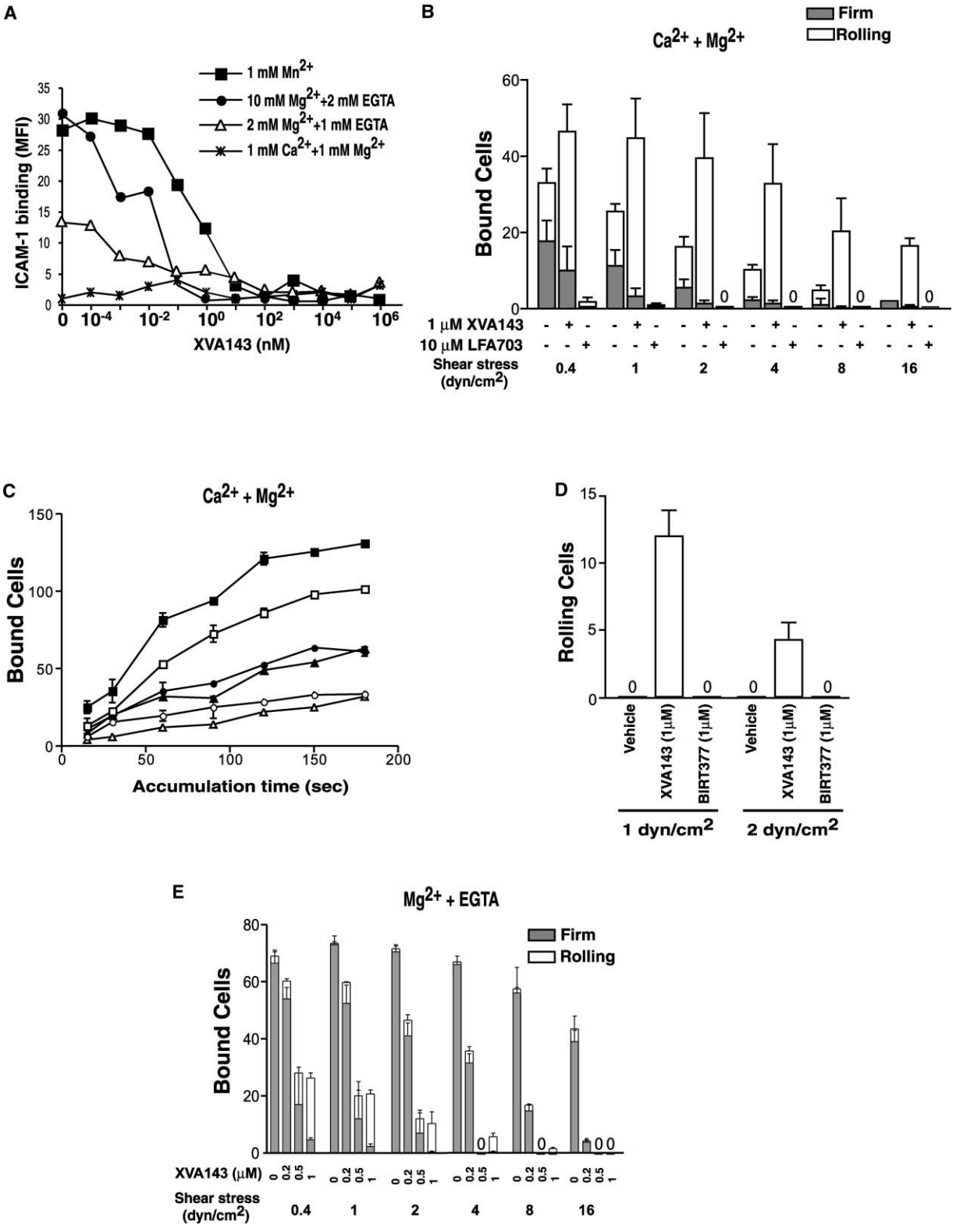

Figure 2. Effect of XVA143 on Binding to ICAM-1

(A) K562 cells expressing $\alpha_L\beta_2$ were incubated with XVA143 in the presence of the indicated divalent cations. Binding of multimeric, soluble ICAM-1 was determined using flow cytometry and expressed as specific mean fluorescence intensity (MFI).

(B) $\alpha_L\beta_2$ K562 cells were prepared in Buffer A/1 mM Ca^{2+}/1 mM Mg^{2+} containing DMSO, 1 μM XVA143, or 10 μM LFA703. Cells were immediately infused into a flow chamber with ICAM-1-Fcγ immobilized on the lower wall. The number of firmly adherent or rolling cells was determined for each shear stress interval. Bars represent the average ± SEM of three to five independent experiments.

If integrin extension is important in supporting rolling, whereas the high-affinity conformation of the α_L I domain is not, then α/β I-like allosteric antagonists should have the paradoxical effect of enhancing rolling adhesion through $\alpha_L\beta_2$. Indeed, in Ca^{2+}/Mg^{2+}, XVA143 markedly increased the total number of $\alpha_L\beta_2$ transfectants that accumulated at 0.3 dyn/cm^2, and remained adherent at 0.4 to 16 dyn/cm^2 (Figure 2B). Furthermore, XVA143 increased the total number of cells that rolled, and decreased the number of cells that were firmly adherent, at all wall shear stresses in Ca^{2+}/Mg^{2+} (Figure 2B). The increase in rollingly adherent cells was particularly marked at 2 to 16 dyn/cm^2 (Figure 2B). The agonistic effect in shear flow of XVA143 was further verified in accumulation assays (Figure 2C). Accumulation at all wall shear stresses tested, 0.4, 0.6, and 0.8 dyn/cm^2, was enhanced by XVA143. In contrast, the α I allosteric antagonists LFA703 and BIRT377, which stabilize the closed conformation of the I domain, and the overall bent conformation of $\alpha_L\beta_2$ (Shimaoka et al., 2003a) greatly decreased the number of interacting cells (Figure 2B; data not shown) (Salas et al., 2002).

Although β_2 integrins clearly contribute to leukocyte rolling in inflamed vessels in vivo (Forlow and Ley, 2001; Forlow et al., 2000; Henderson et al., 2001; Jung et al., 1998; Perry and Granger, 1991), rolling by peripheral blood cells on ICAM-1 substrates has not previously been demonstrated in vitro. Indeed, under control conditions we failed to detect rolling by peripheral blood lymphocytes (PBL) on ICAM-1 substrates (Figure 2D), consistent with the markedly lower expression of LFA-1 on PBL than K562 transfectants (not shown). However, XVA143 treatment induced readily detectable tethering in shear flow and rolling adhesion of PBL on ICAM-1 substrates (Figure 2D). By contrast, the α I antagonist BIRT377 did not induce rolling adhesion (Figure 2D). In Mg^{2+}/EGTA (Figure 2E) and Mn^{2+} (not shown), LFA-1 bearing cells develop firm adhesion to ICAM-1 substrates, with hardly any cells rolling. Addition of increasing concentrations of XVA143 resulted in a decreasing number of firmly adherent cells and an increasing number of rolling cells (Figure 2E). At 1 μM XVA143, almost all of the adherent cells exhibited the rolling modality. At maximally effective XVA143 concentrations of 1 μM, more cells accumulated and rolled in Ca^{2+}/Mg^{2+} than in Mg^{2+}/EGTA (Figure 2B compared to 2E), suggesting that Ca^{2+} makes a contribution to rolling interactions in the XVA143-bound conformation of $\alpha_L\beta_2$. No interactions occurred in Ca^{2+} alone or Ca^{2+} + XVA143 (data not shown).

Contrasting results were obtained in assays of binding of multimeric soluble ICAM-1, which requires high- affinity $\alpha_L\beta_2$. XVA143 completely abolished binding of ICAM-1 to LFA-1 in Mn^{2+} and Mg^{2+}/EGTA, with no hint of agonism (Figure 2A).

Dose Dependence of the Effect of XVA143 on Rolling Stability and Exposure of Activation Epitopes

The IC_{50} values for inhibition by XVA143 of binding of soluble, multimeric ICAM-1 varied depending on the activating divalent cation conditions. XVA143 was most potent against the weakest activator (2 mM Mg^{2+}/1 mM EGTA, IC_{50} $\sim 10^{-3}$ nM) and least potent against the strongest activator (1 mM Mn^{2+}, IC_{50} $\sim$0.3 nM) (Figure 2A). The IC_{50} value for 10 mM Mg^{2+}/1 mM EGTA was intermediate ($\sim 10^{-2}$ nM). All of these IC_{50} values for inhibition of soluble multimeric ICAM-1 binding are in the subnanomolar range. By contrast, in shear flow adhesion assays in Mg^{2+}/EGTA, 500 nM to 1 μM concentrations were required for inhibition of firm adhesion, and for stimulation of rolling adhesion (Figure 2E). This difference may reflect a higher affinity of XVA143 for activated receptors than for resting receptors, as demonstrated for α/β I-like competitive antagonists of integrin $\alpha_{IIb}\beta_3$ (Bednar et al., 1998).

We hypothesized that exposure of activation epitopes and stimulation of rolling adhesion in Ca^{2+}/Mg^{2+} would each involve binding of XVA143 to the low-affinity resting receptor, and therefore should occur in similar concentration ranges. Increasing concentrations of XVA143 markedly stabilized rolling interactions, as shown by a higher number of rolling cells (Figure 3A) and slower rolling velocities (Figure 3B). The effect of XVA143 began at a concentration of about 10 nM and was maximal at about 1 μM. The dose responses were examined for exposure of activation epitopes recognized by mAbs to different $\alpha_L\beta_2$ extracellular domains. mAb KIM127 maps to residues in I-EGF domain 2 of the β_2 subunit (Beglova et al., 2002; Lu et al., 2001a; Robinson et al., 1992). mAb m24 maps to residues that locate near the top of the β_2 subunit I-like domain, not far from its MIDAS (Lu et al., 2001c). The exposure of the KIM127 and m24 epitopes by XVA143 followed a similar dose-response as for stabilization of rolling, with the largest increase in the range of 10 nM to 1 μM (Figure 3C). The EC_{50} values for stabilization of rolling adhesion and induction of activation epitopes each occurred within the range of 10 to 100 nM XVA143 (Figures 3A–3C).

Comparison between mAbs to the α_L I Domain and β_2 I-like Domain for Effect on Adhesive Modality and Global Conformation

Could mAbs also differentially affect firm adhesion as compared to rolling adhesion? TS1/22 Fab to the α_L I domain completely inhibited rolling and firm adhesion in both Ca^{2+}/Mg^{2+} and Mg^{2+}/EGTA (Figure 4). Similarly, the α I allosteric antagonist BIRT377 completely inhibited rolling and firm adhesion in both Ca^{2+}/Mg^{2+} and Mg^{2+}/EGTA (Figure 4), as previously shown for the α I allosteric antagonist LFA703 (Salas et al., 2002). TS1/18

(C) $\alpha_L\beta_2$ K562 cells were resuspended in Buffer A/1 mM Ca^{2+}/1 mM Mg^{2+} in the presence of 0 or 1 μM XVA143. Cells were infused at 0.4, 0.6, or 0.8 dyn/cm^2 into the flow chamber and the number of bound cells (rolling or firmly adherent) determined with time. Filled and open symbols are with and without 1 μM XVA143, respectively; squares, 0.4 dyn/cm^2; circles, 0.6 dyn/cm^2; triangles, 0.8 dyn/cm^2. Average $\pm$ s.e.m. of three experiments.

(D) Freshly isolated human PBMCs resuspended in Buffer A/1 mM Ca^{2+}/1 mM Mg^{2+} in the presence of 1 μM XVA143, 1 μM BIRT377 or the equivalent amount of DMSO were infused at 0.3 dyn/cm^2 and the number of rolling cells was determined at 1 and 2 dyn/cm^2. Bars represent the average $\pm$ SEM of three independent experiments.

(E) As in (B) except in 2 mM Mg^{2+}/1 mM EGTA and the indicated XVA143 concentrations.

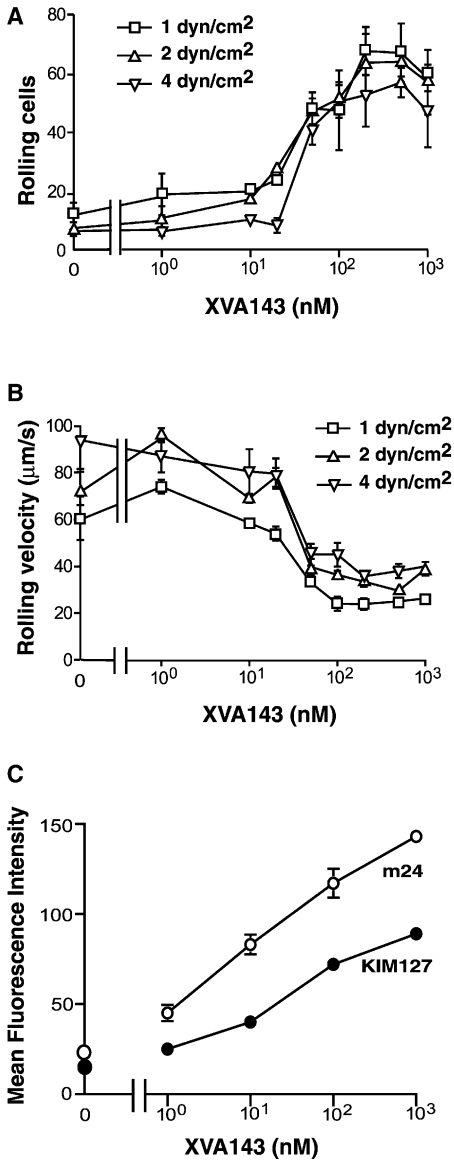

Figure 3. XVA143 Dose-Dependent Stabilization of Rolling Adhesion Mirrors $\alpha_L\beta_2$ Straightening

(A and B) $\alpha_L\beta_2$ K562 cells were resuspended in Buffer A/1 mM Ca^{2+}/1 mM Mg^{2+} in the presence of 0–1000 nM XVA143. Cells were introduced into a flow chamber and allowed to accumulate for 30 s at 0.3 dyn/cm² onto an ICAM-1-Fcγ substrate (see Experimental Procedures). Shear was then increased and the number of rolling cells (A) as well as their rolling velocity (B) was measured at 1, 2, and 4 dyn/cm². Average ± s.e.m. of three experiments.

(C) $\alpha_L\beta_2$ K562 cells in HBS/1 mM Ca^{2+}/1 mM Mg^{2+} were incubated with different concentrations of XVA143. Binding to activation-dependent mAbs KIM127 and m24 was detected by flow cytometry. Exposure of the epitopes at 1,000 nM XVA143 appeared maximal, because it was equivalent to that in 1 mM Mn^{2+}. Average ± s.e.m. of two experiments.

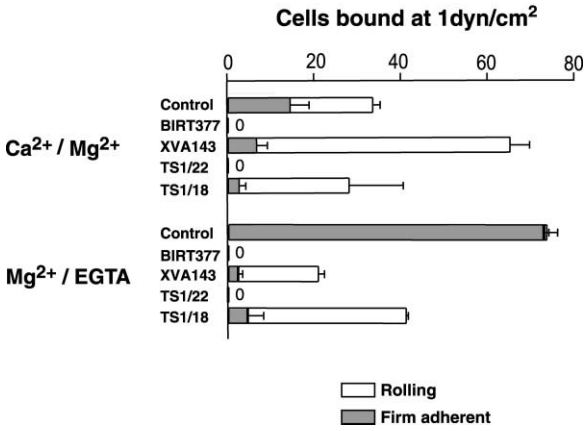

Figure 4. Effect of Different LFA-1 Inhibitors on Rolling on ICAM-1 Substrates

Wild-type $\alpha_L\beta_2$ K562 cells were treated with 10 μg/ml TS1/22 Fab against the α_L I domain, 10 μg/ml TS1/18 Fab to the β_2 I-like domain, 1 μM BIRT377, or 1 μM XVA143 in 1 mM Ca^{2+}/Mg^{2+} or 2 mM Mg^{2+}/1 mM EGTA for 30 min at room temperature, and then accumulated on an ICAM-1-Fcγ-coated substrate at 0.3 dyn/cm². Wall shear stress was incremented every 10 s and the number of rolling and firmly adherent cells measured at 1 dyn/cm². Mean and s.e.m. for three to four experiments.

and other mAbs that bind to the β_2 I-like domain are allosteric inhibitors, since they inhibit ligand binding by wild-type $\alpha_L\beta_2$ but not $\alpha_L\beta_2$ containing an I domain locked in the high-affinity state with a disulfide bond (Lu et al., 2001c). Interestingly, in Ca^{2+}/Mg^{2+} TS1/18 Fab increased the number of rolling cells, while it decreased by a similar amount the number of firmly adherent cells (Figure 4). Furthermore, whereas in Mg^{2+}/EGTA almost all cells were firmly adherent, TS1/18 Fab resulted in an almost complete adhesive phase transition, converting ~90% of the cells to rolling adhesion.

Although TS1/18 Fab and XVA143 each inhibit firm adhesion, they differ in other respects. In Ca^{2+}/Mg^{2+}, TS1/18 Fab did not increase the total number of adherent cells, whereas XVA143 consistently increased the total number of adherent cells (Figure 4). Furthermore, in contrast to XVA143, TS1/18 Fab did not decrease rolling velocity (data not shown). TS1/18 Fab and XVA143 were further compared for their effect on activation epitope exposure (Table 1). Although there was little KIM127 or m24 epitope exposure in Ca^{2+}/Mg^{2+}, pretreatment with TS1/18 Fab further reduced epitope exposure. By contrast, in Ca^{2+}/Mg^{2+} XVA143 markedly increased exposure of both epitopes, and TS1/18 Fab largely and partially reversed this effect of XVA143 for the KIM127 and m24 epitopes, respectively (Table 1). Expression of both epitopes was increased by Mg^{2+}/EGTA and increased further by Mn^{2+}; the increases by Mg^{2+}/EGTA and Mn^{2+} were also markedly reversed by TS1/18 Fab (Table 1). The results point to two mechanisms for enhancing rolling. TS1/18 inhibits firm adhesion, and this appears to explain its enhancement of rolling adhesion, because TS1/18 never increased the total number of adherent cells. By contrast, XVA143 not only inhibits firm adhesion but enhances rolling adhesion, as shown by the increase in total number of adherent cells in Ca^{2+}/Mg^{2+}. This enhancement by XVA143 but not TS1/18 Fab is consistent with induction of the extended conformation by XVA143 but not TS1/18 Fab.

Table 1. Effect of TS1/18 Fab and XVA143 on Exposure of Activation-Dependent Epitopes

	Mouse Fab	TS1/18 Fab	DMSO	XVA143	TS1/18 + XVA143
KIM127					
Ca^{2+} + Mg^{2+}	7.3 ± 0.45	5.2 ± 0.5	9.3 ± 0.7	85.8 ± 1.4	33.2 ± 1.8
Mg^{2+} + EGTA	27.8 ± 3.7	17.6 ± 0.3	21.6 ± 5.0	87.3 ± 2.8	74.7 ± 3.8
Mn^{2+}	48.9 ± 3.3	35.8 ± 2.05	54.2 ± 6.1	75.5 ± 3.6	75.0 ± 3.5
m24					
Ca^{2+} + Mg^{2+}	3.9 ± 1.7	0.2 ± 0.2	5.5 ± 0.9	126.9 ± 0.6	74.2 ± 4.2
Mg^{2+} + EGTA	56.3 ± 7.0	18.1 ± 2.8	44.2 ± 1.8	101.3 ± 11.1	102.1 ± 31.5
Mn^{2+}	127.0 ± 6.3	83.0 ± 11.6	115.8 ± 8.2	144.1 ± 2.1	146 ± 1.3

Binding of KIM127, m24, and control mouse IgG was determined after incubation with 10 μg/ml control mouse Fab or TS1/18 Fab, $1{:}10^5$ dilution of DMSO or 1 μM XVA143 in the presence of the indicated divalent cations. KIM127 and m24 binding was measured with FITC anti-mouse IgG, Fc specific, and background with control mouse IgG was subtracted. Values are specific mean fluorescence intensity of three to four independent experiments ± S.D.

A Single Mutation in the I Domain Linker, E310A, Abrogates Both Integrin Activation and $\alpha_L\beta_2$ Straightening, Resulting in Complete Inhibition of Rolling and Firm Adhesion

Mutation of Glu-310 of α_L to Ala has been shown to abrogate binding of $\alpha_L\beta_2$ to ICAM-1 in a static adhesion assay (Huth et al., 2000). Moreover, this mutant does not respond to activation by an activating mAb (Huth et al., 2000). Residue α_L-Glu-310 locates to the linker that follows the C-terminal α7-helix of the I domain, connects to the β-propeller domain, and must be nearby in the 3-dimensional structure to the MIDAS of the β_2 I-like domain. As proposed (Alonso et al., 2002; Shimaoka et al., 2002), Glu-310 has been demonstrated (Yang et al., 2004b) to function as an intrinsic ligand that binds to the β_2 I-like MIDAS when it is activated, thereby exerting a downward pull on the C-terminal α-helix of the α I domain, and activating its MIDAS. Remarkably, experiments with K562 transfectants, which expressed wild-type and mutant $\alpha_L\beta_2$ at comparable densities as shown with TS2/4 mAb to a constitutively exposed epitope (Figure 5A), showed that the α_L-E310A mutation completely abolished rolling adhesion, firm adhesion, and transient tethering, whether measured in Ca^{2+}/Mg^{2+} (Figure 5B), Mn^{2+} (Figure 5C), Mg^{2+}/EGTA, or low wall shear stresses of 0.3 dyn/cm^2 (data not shown).

Treatment with XVA143 Restores Rolling of the α_L-E310A β_2 Mutant by Inducing Extension of $\alpha_L\beta_2$

Despite the complete absence of adhesive interactions by the α_L-E310A mutant, treatment of this mutant with XVA143 restored its ability to support rolling at all wall shear stresses tested (Figure 5B). The complete lack of adhesion of the α_L-E310A mutant in Mn^{2+} (Figure 5C) was in excellent agreement with the observation that Mn^{2+} induced KIM127 epitope exposure in wild-type but not α_L-E310A mutant $\alpha_L\beta_2$ (Figure 5A). Similarly, induction of rolling by XVA143 of the α_L-E310A mutant was in agreement with induction by XVA143 of KIM127 exposure in the α_L-E310A mutant as efficiently as with wild-type $\alpha_L\beta_2$ (Figure 5A). The S114A mutation in the β_2 I-like domain has previously been shown to abolish all tested effects of α/β I-like allosteric antagonists, suggesting that the β_2 I-like domain MIDAS is part of the binding site for these compounds (Shimaoka et al., 2003a). Additionally, the β_2-S114A mutation completely abolished XVA143-induced rolling (Figure 5B) and KIM127 epitope exposure, i.e., extension (Figure 5A).

Regulation of Integrin Extension by α_L I and β_2 I-like Interdomain Communication

Overall, the data suggest that communication between the I domain linker and the I-like domain MIDAS is not only crucial for stabilizing the high-affinity conformation of the I domain, but also regulates the equilibrium between the bent and extended $\alpha_L\beta_2$ conformers. These interactions are important in Ca^{2+}/Mg^{2+} as well as Mn^{2+}, and appear to explain the complete absence in Ca^{2+}/Mg^{2+} of rolling interactions in the α_L-E310A and β_2-S114A mutants (Figure 5B). In support of the suggestion that in the absence of interactions between the α_L linker and β_2 I-like domains, $\alpha_L\beta_2$ is locked in a bent conformation with virtually no equilibration to the extended conformation, the α_L-E310A and β_2-S114A mutants reproducibly showed in three of three experiments lower basal binding in Ca^{2+}/Mg^{2+} of KIM127 mAb than wild-type transfectants (Figure 5A).

To further test the role of α_L-Glu-310 in interdomain communication and ligand binding in $\alpha_L\beta_2$, its influence on ligand-induced exposure of the KIM127 and m24 epitopes was examined. In the presence of control human IgA complexes with anti-IgA, wild-type $\alpha_L\beta_2$ transfectants showed significantly more basal binding of KIM127 mAb than α_L-E310A β_2 transfectants (Figure 6A), confirming that the E310A mutation pushed the equilibrium between the bent and extended conformations toward the bent conformation with no KIM127 epitope exposure. As shown above (Figure 2A), in Ca^{2+}/Mg^{2+}, binding of 20 μg/ml sICAM-1-Fcα complexed with FITC anti-IgA to wild-type $\alpha_L\beta_2$ was only moderately above background. Coupling of ligand binding to the KIM127 and m24 epitopes was examined using a high concentration of 100 μg/ml sICAM-1-Fcα complexed with anti-IgA and coincubation with KIM127 or m24 mAb followed by FITC anti-mouse IgG (Figure 6). For wild-type $\alpha_L\beta_2$, multimeric ICAM-1 increased both KIM127 epitope exposure ($p < 0.05$) and m24 epitope exposure ($p < 0.0005$), demonstrating ligand binding and its coupling to conformational change. By contrast, multimeric ICAM-1 had no effect on epitope exposure in mutant α_L-E310A β_2 integrins. This experiment confirms that the equilibria relating ligand binding and exposure of

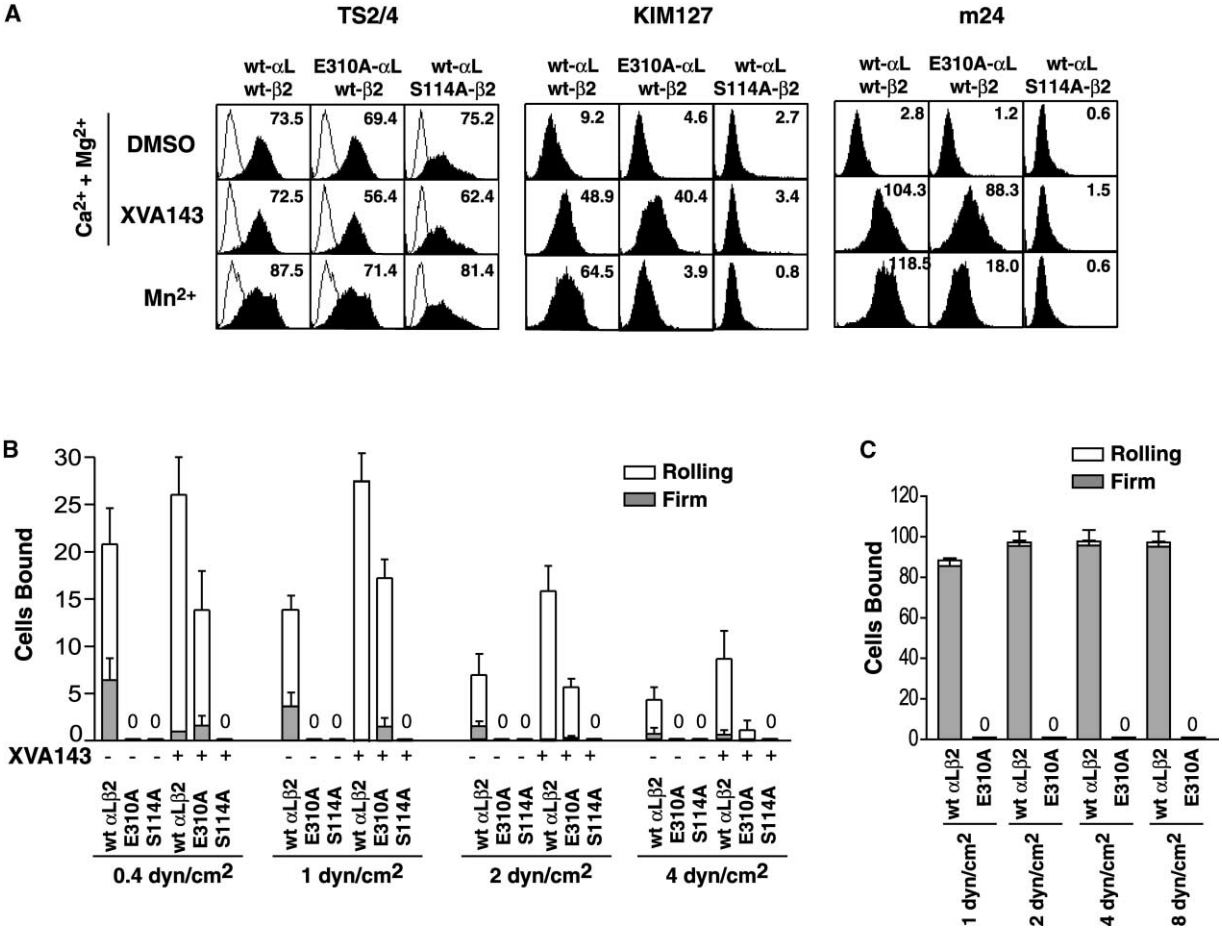

Figure 5. Straightening of α_L-E310A β_2 by XVA143 Restores Rolling Interactions under Flow

(A) K562 cells expressing wt $\alpha_L\beta_2$, α_L-E310A β_2, or $\alpha_L\beta_2$-S114A were incubated with 1 μM XVA143 or an equivalent concentration of DMSO in HBS/Ca^{2+} + Mg^{2+}, or HBS/Mn^{2+}. Binding of a control mouse IgG (open curves), the α_L activation-independent mAb TS2/4, or the β_2 activation-dependent mAbs KIM127 or m24 (closed curves) was detected using flow cytometry. Numbers in the panels are the mean specific fluorescence intensities (averages of three experiments).

(B) K562 cells expressing wt $\alpha_L\beta_2$, α_L-E310A β_2, or $\alpha_L\beta_2$-S114A were incubated in HBS/Ca^{2+} + Mg^{2+} with 1 μM XVA143 or the equivalent concentration of DMSO. Cells were allowed to accumulate over an ICAM-1-Fcγ-coated substrate at 0.3 dyn/cm^2, and the flow rate was increased every 10 s. The number of cells bound, either firmly adherent or rolling, was analyzed at different wall shear stresses.

(C) Same as (B), except in 1 mM Mn^{2+}. Data are mean ± s.e.m. of three experiments.

KIM127 and m24 epitopes are coupled through α_L residue Glu-310, and does not define whether affinity for ICAM-1, extension, or both are affected. Binding of control IgG or TS2/4 (an activation-independent β-propeller mAb) was unchanged by incubation of multimeric ICAM-1 with wild-type $\alpha_L\beta_2$ or mutant α_L-E310A β_2 (data not shown).

XVA143 Treatment Increases the Fraction of Murine Lymphocytes that Roll in Lymph Node Microvessels, and Decreases the Speed at which They Roll

Physiological lymphocyte rolling in peripheral lymph node high endothelial venules (HEV) is mediated primarily by L-selectin binding to its endothelial ligand, peripheral node addressin (PNAd), while the chemokine-triggered binding of activated $\alpha_L\beta_2$ to endothelial ICAM-1 leads to subsequent firm adhesion (von Andrian and Mackay, 2000). Intravital microscopy (IVM) in mouse inguinal lymph nodes was used to test the effects of XVA143 on lymphocyte rolling and firm adhesion in vivo. Treatment of wild-type murine lymphocytes with 100 μM XVA143 induced a 50% increase in rolling fraction compared to vehicle-treated control cells (from 27 ± 5% to 41 ± 7%) (Figure 7A). This effect of XVA143 was largely eliminated by antibody blockade of $\alpha_L\beta_2$ function (Figure 7A). Cooperation with L-selectin was required for detection of LFA-1-dependent, XVA143-enhanced lymphocyte rolling, because XVA143-treated lymphocytes from L-selectin$^{-/-}$ mice did not roll in HEV (data not shown). Lymphocytes treated with XVA143 rolled at a markedly slower velocity than cells treated with DMSO vehicle (Figure 7B). Again, this effect of XVA143 was completely reversed by LFA-1 mAb (Figure 7B). The effects on lymphocyte rolling velocity were highly significant (Figure 7 legend). These effects were not due to changes in microvascular hemodynamics between treatment groups (data not shown). Despite the substan-

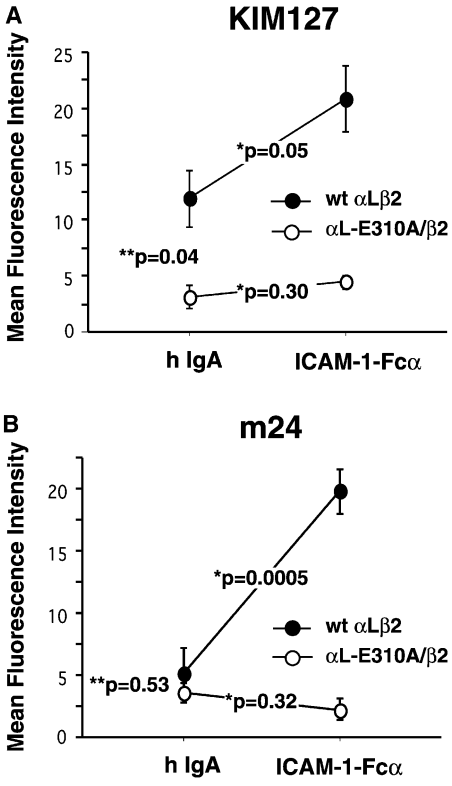

Figure 6. Induction of Activation-Dependent Epitope Exposure by Multimeric ICAM-1

K562 cells expressing wt or $\alpha_L\beta_2$ α_L-E310A β_2 in HBS/Ca^{2+}/Mg^{2+} were incubated with ICAM-1-Fcα/goat anti-human IgA or human IgA/goat anti-human IgA in the presence of control IgG, TS2/4, m24, or KIM127 mAbs. Binding of the mAbs was detected by FITC-anti-mouse IgG antibody. Binding of control mouse IgG or mAb TS2/4 was unchanged by the presence of multimeric ICAM-1 (not shown). Data are mean ± s.e.m. of three to five experiments. *, p value of IgA versus ICAM-1-Fcα. **, p value of wild-type $\alpha_L\beta_2$ versus α_L-E310 β_2.

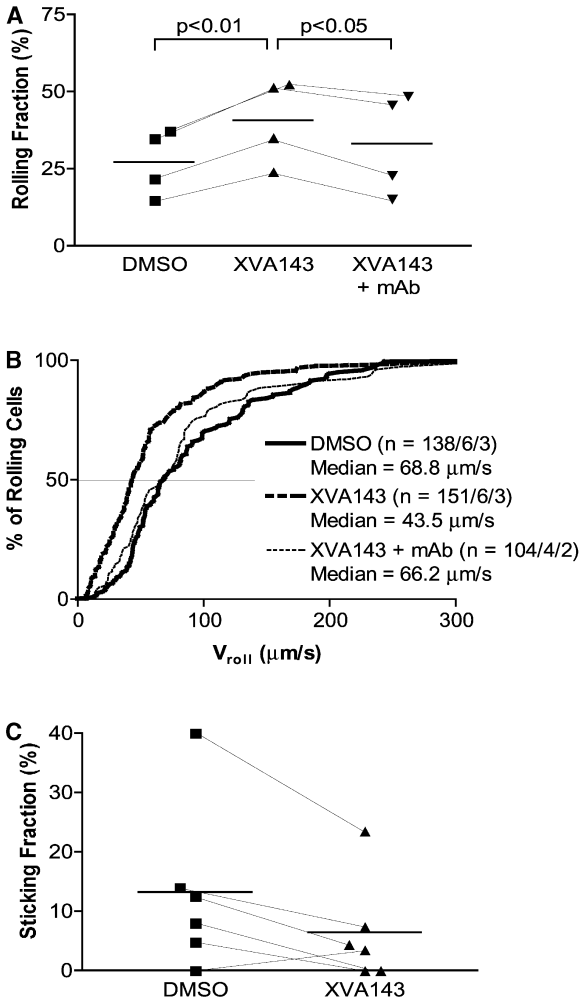

Figure 7. Effects of XVA143 on Intravascular Lymphocyte Adhesion in Lymph Node HEV

(A) Rolling fraction of wild-type lymphocytes treated with DMSO, XVA143, or XVA143 plus anti-α_L or anti-β_2 antibody (XVA143 + mAb). The different cell samples were sequentially injected into P-selectin$^{-/-}$ recipient mice and their rolling behavior in HEV was analyzed (n = 2 mice). Rolling fractions of each lymphocyte sample within the same HEV are identified by symbols connected by straight lines. Means are shown as horizontal lines. Statistical differences were evaluated using repeated measurements ANOVA with Bonferroni correction.

(B) Cumulative velocity curves of rolling cells. Individual rolling velocities are plotted against the percentage of rolling cells moving at or below that velocity. The number (n) of cells/venules/mice that were analyzed for each group is shown in parentheses. Statistical differences, evaluated using the nonparametric Kruskal-Wallis/Dunn's Multiple Comparison test, were as follows: DMSO versus XVA143, $p < 0.001$; XVA143 versus XVA143 + mAb, $p < 0.001$; DMSO versus XVA143 + mAb, $p > 0.05$ (not significant).

(C) Sticking fraction of lymphocytes treated with DMSO or XVA143 in lymph node HEV of mice treated as in A (n = 3 mice). Differences between mean values (horizontal lines) did not reach statistical significance ($p = 0.059$; paired Student's t test).

tial reduction in rolling velocity induced by XVA143, the fraction of rolling cells that became firmly adherent was markedly reduced from 13 ± 5% to 6 ± 3%. The differences in the sticking fraction between XVA-treated and DMSO-treated lymphocytes were almost statistically significant ($p = 0.059$; Figure 7C).

Discussion

β_2 integrins and $\alpha_L\beta_2$ especially are best known for supporting firm leukocyte adhesion to endothelium and transendothelial migration. Nonetheless, as reviewed in the Introduction, there is extensive in vivo evidence that β_2 integrins including $\alpha_L\beta_2$ also contribute to rolling adhesion by neutrophils, by affecting the efficiency of accumulation of rolling cells or the velocity of rolling cells. How can β_2 integrins mediate both rolling and firm adhesion, which can be viewed as phases, analogously to the liquid and crystalline states, with markedly different requirements for receptor-ligand bond formation and dissociation kinetics? Here, we demonstrate that distinct conformational states of $\alpha_L\beta_2$ regulate rolling and firm adhesion, and that an extended conformation of $\alpha_L\beta_2$ favors rolling. Furthermore, we demonstrate that the overall conformation of $\alpha_L\beta_2$ and its ability to support rolling are regulated by interactions between the α_L I

and β_2 I-like domains, and make the surprising observation that an α/β I-like allosteric integrin antagonist can inhibit firm adhesion and enhance or induce rolling adhesion.

The findings with XVA143 demonstrate that rolling is induced by $\alpha_L\beta_2$ extension in the absence of activation of high-affinity ligand binding by the I domain. In Ca^{2+}/Mg^{2+}, XVA143 enhanced the number of cells rolling through LFA-1 both by increasing the rate of accumulation of cells in shear flow and hence the total number of adherent cells, and also by inhibiting firm adhesion through LFA-1. Mg^{2+}/EGTA and Mn^{2+} activate firm adhesion through $\alpha_L\beta_2$. In Mg^{2+}/EGTA, XVA143 altered the phenotype from firm adhesion to rolling adhesion. Comparison between XVA143-treated cells in Mg^{2+}/Ca^{2+} and Mg^{2+}/EGTA shows that Ca^{2+} enhances the stability of rolling interactions. Ca^{2+} is also important for rolling interactions through α_4 integrins (de Chateau et al., 2001) and stabilizes the ADMIDAS of integrin $\alpha_4\beta_7$ in a conformation that supports rolling (Chen et al., 2003). Peripheral blood lymphocytes failed to mediate rolling on ICAM-1 substrates, consistent with the absence to date of any publications demonstrating rolling solely through β_2 integrin-ICAM-1 interactions by peripheral blood leukocytes. However, XVA143 treatment enabled LFA-1 on PBL to mediate tethering and rolling in shear flow on ICAM-1 substrates. Together with our in vivo studies, this demonstrates that the physiological density of $\alpha_L\beta_2$ on PBL is sufficient to contribute to rolling, when the conformation of LFA-1 is appropriate.

Direct observations on integrin conformation have thus far come from crystal, EM, and X-ray scattering studies on integrins that lack I domains (Adair and Yeager, 2002; Mould et al., 2003a; Takagi et al., 2002, 2003; Xiong et al., 2001, 2002). Three conformations have been revealed for $\alpha_V\beta_3$ (Figures 1F–1H), and similar conformations have been suggested for the I domain-containing integrin $\alpha_L\beta_2$ (Beglova et al., 2002; Takagi et al., 2002) (Figures 1A–1E). XVA143 induces exposure of the KIM127 epitope in I-EGF module 2, strongly suggesting conversion of $\alpha_L\beta_2$ from a bent to an extended conformation. In Mn^{2+} or Mg^{2+}/EGTA, XVA143 blocked soluble, multimeric ICAM-1 binding at subnanomolar concentrations. However, in Ca^{2+}/Mg^{2+}, XVA143 induced accumulation of rolling cells, a decrease in rolling velocity, and an increase in KIM127 and m24 epitopes, with half-maximal effects between 10 and 100 nM. The finding that XVA143 induces both rolling and integrin extension as measured by KIM127 epitope exposure, and that the dose-response is similar, strongly supports a direct relationship between the extension of LFA-1 and its enhanced ability to support adhesion in shear flow and rolling.

In vivo data suggest that β_2 integrins and LFA-1 on neutrophils contribute to rolling interactions in inflamed venules (Forlow and Ley, 2001; Forlow et al., 2000; Henderson et al., 2001; Jung et al., 1998; Perry and Granger, 1991), whereas LFA-1 on lymphocytes does not contribute to lymphocyte rolling interactions in uninflamed HEV (Warnock et al., 1998). The latter result is confirmed by our findings, but we also demonstrate that when the extended conformation of LFA-1 with a low-affinity I domain is induced by XVA143, it enhances rolling interactions in HEV. Differences in the contribution of LFA-1 to rolling in vivo may reflect differences in regulation of LFA-1 between lymphocytes or neutrophils, or differences in the concentration and duration of exposure to activating stimuli such as chemokines in inflamed tissues and HEV. Although lower rolling velocity is usually associated with a higher fraction of cells that become firmly adherent, XVA143 markedly decreased the fraction that became firmly adherent in HEV. This finding is in agreement with in vitro observations that XVA143 enhances rolling adhesion while blocking firm adhesion. The effect on firm adhesion in vivo fell short of statistical significance; however, we caution that the pharmacokinetics of XVA143 or any other α/β I-like allosteric antagonist are not yet published, and we do not know if XVA143 remained saturating in vivo.

Recently, a "humanized" mAb to the LFA-1 I domain has been approved by the FDA for treatment of moderate to severe psoriasis (Gordon et al., 2003), and α/β I-like allosteric antagonists have been proposed as small molecule follow-ons to this antibody (Gadek et al., 2002). We have shown that a mAb to the α_L I domain blocks both firm adhesion and rolling adhesion, whereas α/β I-like allosteric antagonists of LFA-1 block firm adhesion while inducing or enhancing rolling adhesion. Because of the importance of firm adhesion by β_2 integrins, this difference in mechanism of action certainly does not preclude the therapeutic utility of α/β I-like allosteric antagonists; however, it does need to be taken into account during preclinical and clinical development. Furthermore, attention should be paid in medicinal chemistry to the difference in potency between blocking high-affinity ligand binding and inducing rolling adhesion, which likely reflects a higher affinity of these antagonists for the active conformation of the β_2 I-like domain. It might be possible to find compounds that differ in the ratios of the IC_{50} values for different conformational states of β_2 integrins, as has been demonstrated for α/β I-like competitive antagonists of $\alpha_{IIb}\beta_3$ (Bednar et al., 1998).

The TS1/18 Fab has a different mechanism of action from XVA143. TS1/18 did not induce rolling by PBL or enhance adhesion in shear flow to ICAM-1 substrates. However, TS1/18 almost completely switched the adhesive phenotype from firm or mixed adhesion to rolling adhesion. Consistent with lack of enhancement of adhesiveness by TS1/18 Fab, it did not increase KIM127 epitope expression. Rather, TS1/18 appears to stabilize the inactive conformation of the β_2 I-like domain, inhibiting firm adhesion and enabling rolling adhesion to occur instead.

Overall, the results with XVA143 and TS1/18 Fab suggest that extension of $\alpha_L\beta_2$ favors adhesion, and that the conformation of the β_2 I-like domain regulates the affinity of the α_L I domain and whether it mediates rolling adhesion or firm adhesion. Previous studies on mutant I domains expressed as isolated α_L I domains with an artificial transmembrane domain or within intact $\alpha_L\beta_2$ heterodimers have shown that the wild-type, unconstrained α_L I domain mediates rolling, whereas the α_L I domain locked in the high-affinity conformation mediates only firm adhesion (Salas et al., 2002). This finding suggests that XVA143 and TS1/18 each block firm adhesion by blocking the conversion of the α_L I domain to the high-affinity conformation, although they do so by

different mechanisms because XVA143 enhances while TS1/18 Fab inhibits induction of the m24 epitope in the β_2 I-like domain. In terms of currently understood integrin conformations, the conformation mediating rolling appears to most closely correspond to $\alpha_L\beta_2$ in an extended conformation with a low-affinity I domain (Figures 1B and 1C), whereas the conformation that mediates firm adhesion appears to most closely correspond to an extended conformation with a high- affinity α_L I domain (Figure 1E).

The studies with XVA143 and the α_L-E310A mutation yield insights into communication between the α_L I and β_2 I-like domains and how it regulates global conformation and rolling. The α_L-Glu-310 residue in the linker between the α_L subunit I and β-propeller domains appears to bind to the β_2 I-like MIDAS when it is activated, and through displacement of the C-terminal α-helix of the I domain, to transduce activation to the I domain MIDAS (Alonso et al., 2002; Shimaoka et al., 2002; Yang et al., 2004b). We found that the α_L-E310A mutation not only blocked firm adhesion, but also completely blocked rolling adhesion through $\alpha_L\beta_2$. Expression under basal conditions of the KIM127 epitope was significantly decreased, demonstrating coupling of residue α_L-Glu-310 in the α_L I domain-β-propeller linker to a distal site in the 3-dimensional structure in I-EGF2 in the β_2 genu. These results suggest that under basal conditions, some equilibration between the bent and extended structures occurs, i.e., breathing at the β_2 genu, and that this breathing is linked to α_L residue Glu-310, possibly by an interaction of this residue with the β_2 I-like domain MIDAS. Furthermore, the mutation α_L-E310A completely abolished increase by soluble, multimeric ICAM-1 of the m24 and KIM127 epitopes, demonstrating either that linkage through α_L-Glu-310 is required for the I domain to have sufficient affinity to bind ligand, or that this linkage is required for ligand binding by the I domain to be communicated to the β_2 I-like domain and the genu.

Remarkably, XVA143 rescued the negative effect of the α_L-E310A mutation on rolling adhesion. Whereas the α_L-E310A mutation abolished rolling adhesion, addition of XVA143 restored rolling almost to wild-type levels, and induction of the m24 and KIM127 epitopes was similar to wild-type. These results further emphasize the importance of the extended integrin conformation for rolling adhesion. They suggest that the α_L-E310A β_2 heterodimer is in a conformation incapable of supporting rolling, likely because it is in the bent conformation and does not appreciably equilibrate with the extended conformer, as suggested by the lower expression of the KIM127 epitope on α_L-E310A β_2 than wild-type $\alpha_L\beta_2$ transfectants.

XVA143 was completely unable to rescue rolling by the β_2 I-like MIDAS mutant S114A, or as previously described for this mutant, m24 and KIM127 epitope expression (Shimaoka et al., 2003a). This supports the previous conclusion that XVA143 and related α/β I-like antagonists utilize as part of their binding site the β_2 I-like domain MIDAS. The efficacy of XVA143 with the α_L-E310A mutant demonstrates that α_L-Glu-310 is not an important part of the XVA143 binding site, and is consistent with the model that XVA143 is a mimic of α_L-Glu-310 and inhibits its binding to the β_2 I-like MIDAS.

In contrast to XVA143, Mn^{2+} did not induce straightening of the α_L-E310A mutant as shown by lack of induction of the KIM127 epitope, and the mutant was completely incapable of interactions in shear flow in Mn^{2+}. Mn^{2+} is a strong activator of wild-type $\alpha_L\beta_2$, inducing opening of the I-like domain as measured with m24 mAb, extension of the integrin as measured with KIM127 mAb, and firm adhesion. Mn^{2+} activates by binding to the I-like domain ADMIDAS, as recently demonstrated with the $\alpha_4\beta_7$ integrin (Chen et al., 2003). Together with the positive control of the effect of XVA143 on the α_L-E310A mutant, these results suggest that Mn^{2+} activates adhesiveness of the α_L I domain through interaction of α_L-Glu-310 with the I-like domain. The results further demonstrate that the interaction through α_L-Glu-310 activated by Mn^{2+} is required for $\alpha_L\beta_2$ extension as measured by KIM127 exposure. Some induction of m24 expression in the I-like domain by Mn^{2+} is noted in the α_L-E310A mutant, although it is markedly attenuated compared to wild-type. This is consistent with the ability of Mn^{2+} to bind to the β_2 I-like domain and partially stabilize localized conformational change, with a partial requirement for linkage through α_L-Glu-310 to stabilize this altered local conformation, and a complete requirement for α_L-Glu-310 for linkage of local, weak effects of Mn^{2+} to the α_L I domain and exposure of the KIM127 epitope in β_2 I-EGF module 2.

In summary, our results show that $\alpha_L\beta_2$ mediates rolling when it is in an extended conformation and the α_L I domain is not in a high-affinity state. We demonstrate that equilibration between a bent conformation in which the KIM127 epitope is buried and an extended conformation in which the KIM127 epitope is exposed, i.e., breathing at the headpiece-tailpiece interface, is important for rolling interactions mediated by $\alpha_L\beta_2$. The interface between the I domain linker region and the I-like domain functions as a switch that can regulate the affinity of the α_L I domain as well as the switchblade-like extension of $\alpha_L\beta_2$. In vivo, $\alpha_L\beta_2$ is sufficient by itself to support firm adhesion, and can contribute in combination with other adhesion receptors to rolling adhesion. We demonstrate that a small molecule antagonist can induce rolling adhesion through $\alpha_L\beta_2$, and that distinct conformational states of $\alpha_L\beta_2$ mediate rolling adhesion and firm adhesion. This raises the intriguing possibility that in vivo, distinct conformational states of $\alpha_L\beta_2$ may also be responsible for supporting rolling and firm adhesion. This could occur if intermediate levels of activating stimuli induced an intermediate conformation of LFA-1 that was extended but did not have a fully activated I domain, as depicted in Figures 1B and 1C. Analogous intermediate states of $\alpha_V\beta_3$ have been directly observed (Figure 1G). A novel intermediate conformational state of the α_L I domain has recently been demonstrated structurally, further emphasizing the complexity of the regulation of $\alpha_L\beta_2$ (Shimaoka et al., 2003b).

Experimental Procedures

Cell Lines, Antibodies, and Small Molecules

K562 cells stably transfected with wild-type $\alpha_L\beta_2$ were described previously (Lu et al., 2001b). α_L-310A and β_2-S114A mutants and $\alpha_L\beta_2$ K562 transfectants were as described (Shimaoka et al., 2003a). Similar $\alpha_L\beta_2$ surface expression as wild-type was routinely verified by immunofluorescence flow cytometry. The mouse anti-human α_L

mAbs TS2/6 (Huang and Springer, 1997) and MHM24 (DAKO; Carpinteria, CA), anti-β_2 Fab TS1/18, and anti-α_L Fab TS1/22 (Sanchez-Madrid et al., 1982), and matching isotype IgG or Fab controls were used to block LFA-1-mediated interactions. A nonbinding mouse IgG1 (X63) control, anti-human α_L mAbs, TS1/11, TS1/12, TS2/4, and anti-β_2 mAb TS1/18 (all IgG1) were used in immunofluorescent flow cytometry (Lu et al., 2001a; Lu and Springer, 1997). Activation-dependent mAbs KIM127 (Robinson et al., 1992) and m24 (Dransfield and Hogg, 1989; Lu et al., 2001c) were kindly provided by M. Robinson (Celltech, Slough, U.K.) and N. Hogg (Imperial Cancer Research Fund, London), respectively. Purified azide-free, low endotoxin anti-mouse CD11a and anti-mouse CD18 (anti-α_L, M17/4; anti-β_2, GAME46; BD Pharmingen, San Diego, CA) were used in intravital microscopy experiments. XVA143 (Welzenbach et al., 2002) was from Dr. Paul Gillespie, Roche, Nutley, NJ. BIRT377 (Last-Barney et al., 2001) was from Dr. Terence Kelly, Boehringer Ingelheim Pharmaceuticals Inc., Ridgeway, CT. LFA703 (Weitz-Schmidt et al., 2001) was from Dr. G. Weitz-Schmidt, Novartis Pharma AG (Basel, Switzerland).

Production of Fab

Fab fragments of mouse IgG (control) and mAbs TS1/22 and TS1/18 were prepared via papain cleavage using the ImmunoPure Fab Preparation Kit (Pierce; Rockford, IL) according to the manufacturer's instructions, and used to block adhesion at 10 or 20 μg/ml, which was saturating for the specific Fab.

Peripheral Blood Lymphocytes

Peripheral blood mononuclear cells were prepared by Ficoll-Hypaque centrifugation (Ulmer and Flad, 1979). Monocytes were depleted by diluting mononuclear cells from 43 ml blood in 60 ml of Hank's balanced salt solution supplemented with 1% human serum albumin and 20 mM Hepes (pH 7.2) (HHBS-HSA) supplemented with 1 mM Ca^{2+}/Mg^{2+} and plating in three gelatin-coated 150 mm cell culture dishes at 37°C for 45 min. The nonadherent lymphocytes were then recovered, pelleted, and resuspended in HBSS-HSA and used in flow chamber experiments.

Soluble ICAM-1 Binding Assay

Cells were harvested, washed with HBS (20 mM HEPES and 150 mM NaCl [pH 7.3]), and incubated with XVA143 (10^{-4} to 10^6 nM in DMSO) or DMSO alone (1:10^{12} to 1:10^2 dilution) for 15 min at room temperature (22°C). A mixture of 20 μg/ml of IC1-5/IgA chimera containing the five Ig domains of human ICAM-1 fused to the Fc portion of IgA (ICAM-1-Fcα) (Martin et al., 1993) and 25 μg/ml of affinity-purified goat anti-human IgA antibody labeled with FITC (Zymed) was then added to an equal volume (25 μl) of cells and incubated for 30 min at room temperature. Cells were spun down and resuspended in 2% paraformaldehyde in PBS. Fluorescence was detected using flow cytometry.

Binding of Activation-Dependent mAbs in the Presence of sICAM-1

Wt or α_L-E310A β_2 transfected K562 cells were resuspended in HBS/1 mM Ca^{2+} + 1 mM Mg^{2+}. The cell pellet was incubated with a mixture of 100 μg/ml of human IgA or ICAM-1-Fcα and 333 μg/ml of affinity purified goat anti-human IgA antibody for 15 min at 37°C. Thereafter, mouse isotype control IgG, TS2/4, m24, or KIM127 in HBS/ Ca^{2+} + Mg^{2+} was added at 3 μg/ml for 30 min at 37°C. Cells were washed and stained with a FITC-goat anti-mouse IgG for 30 min at 4°C. After washing, cells were fixed with 2% paraformaldehyde and subjected to immunofluorescence flow cytometry.

Cell Adhesion to Immobilized ICAM-1 under Shear Flow

A chimera containing the five Ig domains of human ICAM-1 fused to the Fc portion of IgG (ICAM-1-Fc) at 10 or 60 μg/ml in PBS and 20 mM bicarbonate (pH 9.0) (Coating Buffer) for K562 transfectants and PBL, respectively, was spotted on a dish previously coated with 20 μl (20 μg/ml) protein A (Zymed; San Francisco, CA) in Coating Buffer and blocked with 2% human serum albumin (HSA). ICAM-1 substrates were assembled as the lower wall in a parallel-wall flow chamber and mounted on an inverted phase-contrast microscope (Lawrence and Springer, 1991). Cells were washed twice with Ca^{2+}/Mg^{2+}-free HBSS/10 mM Hepes (pH 7.4)/5 mM EDTA/0.5% bovine serum albumin (BSA), resuspended at 5 × 10^6/ml in Ca^{2+}/Mg^{2+}-free HBSS/10 mM Hepes/0.5% BSA (buffer A), and kept at room temperature (22°C) throughout the experiment. Cells were diluted to 5 × 10^5/ml in buffer A containing 1 mM Ca^{2+} + 1 mM Mg^{2+} or 2 mM Mg^{2+} + 1 mM EGTA, immediately before infusion in the flow chamber using an automated syringe pump. Cells were incubated with XVA143 (1 μM in DMSO), DMSO alone, or mAbs (as IgG or Fab fragments) at saturating concentrations, for 15 min at room temperature. Images were captured using a CCD camera mounted on an inverted microscope with a 10×-objective and recorded on Hi-8 videotape.

Quantification of Interactions under Increasing Shear Forces

Cells were allowed to accumulate at 0.3 dyn/cm^2 for 30 s. Shear stress was then increased to 0.4 dyn/cm^2 and incremented every 10 s up to 36 dynes/cm^2. Rolling velocity at each shear stress was calculated from the average distance traveled by rolling cells in 3 s. The number of cells interacting for more than 3 s with the coated surface was measured at each shear stress. To avoid confusing rolling with small amounts of movement due to tether stretching or measurement error, a velocity of 1.5 μm/s, which corresponds to a movement of 1/2 cell diameter during the 3 s measurement interval, was the minimum velocity required to define a cell as rolling instead of firmly adherent.

Accumulation of Cells under a Fixed Shear Force

Cells were prepared as described above, resuspended in buffer A containing 1 mM Ca^{2+} + 1 mM Mg^{2+}, and as indicated 1 μM XVA143. The cells were infused into the flow chamber, and immediately subjected to a fixed wall shear stress. The number of cells bound (rolling or firm adherent) was determined at different time points.

Statistical Analysis

Data were analyzed when indicated using Student's unpaired t test. Values are reported as mean ± SEM. Statistical significance was defined as $p < 0.05$.

Intravital Microscopy

WT and L-selectin-deficient (L-selectin$^{-/-}$) mice on a mixed C57/B6 × 129 background were used as lymphocyte donors, and P-selectin-deficient mice (P-selectin$^{-/-}$; also on a C57/B6 × 129 background) were used as recipients in intravital microscopy experiments (Weninger et al., 2000). Mice were housed in a specific pathogen-free and viral antibody-free (SPF/VAF) facility at Harvard Medical School. All in vivo procedures complied with NIH guidelines for the care and use of laboratory animals and were approved by the Committees on Animals of both Harvard Medical School and the CBR Institute for Biomedical Research.

Young adult P-selectin$^{-/-}$ mice (6–8 weeks of age) were anaesthetized intraperitoneally with a mixture of ketamine (5 mg/ml) and xylazine (1 mg/ml) in physiological saline. P-selectin$^{-/-}$ mice were used as recipients in order to exclude potential contributions of platelet or endothelial P-selectin to lymphocyte rolling in high endothelial venules (HEV) (Diacovo et al., 1998). Surgical preparation and intravital microscopy of the superficial inguinal (subiliac) lymph node (LN) microvasculature were as described (von Andrian, 1996).

Lymphocytes obtained from pooled peripheral (axillary, brachial, and inguinal) and mesenteric lymph nodes were labeled with calcein AM (final concentration, 60 μM), resuspended in HBSS with 1 mM Ca^{2+} and 1 mM Mg^{2+}, and treated with either DMSO, 100 μM XVA143, or 100 μM XVA143 and 50 μg blocking anti-α_L or anti-β_2 antibody at 37°C for at least 10 min. Small boluses of control lymphocytes were then injected intra-arterially and their adhesive behavior in LN HEV was recorded. Subsequently, recipient mice were given intra-arterial injections of XVA143 (10 μl of 100 μM), and XVA143-treated cells were injected and recorded passing through the same microvessels. In two experiments, recipient mice were then treated with either anti-α_L or anti-β_2 antibody (50 μg) and XVA143 plus antibody-treated cells were injected. Labeled cells were visualized via epifluorescence (von Andrian and M'Rini, 1998).

Interactions between circulating cells and lymph node HEV were analyzed from recorded video images. The rolling fraction for each HEV was calculated as the percentage of labeled cells rolling on the endothelial surface among all labeled cells passing through the HEV. The sticking fraction was calculated as the percentage of cells arresting for >30 s among all rolling cells. Distances traversed by

rolling cells were measured using frame-by-frame video image analysis with specialized software (VVelocity Spatial Correlation Velocimeter, A.R. Preis, Berlin), and then divided by the elapsed time to obtain average rolling velocities (v_{roll}). Cumulative velocity curves were as described (Stein et al., 1999).

Means are given ± SEM. Statistical differences between two data sets were analyzed by paired or unpaired two-tailed Student's t tests, as indicated. Differences between multiple data sets assuming Gaussian distributions (e.g., rolling fraction) were analyzed by repeated measurements ANOVA with Bonferroni correction. For multiple data sets with non-Gaussian distributions (e.g., rolling velocities), the nonparametric Kruskal-Wallis/Dunn's Multiple Comparison test was used.

Acknowledgments

We would like to thank Chris Carman and Wei Yang for reagents. The work was supported by NIH grants HL-48675 (T.A.S.), HL-54936, and AR-42689 (U.H.V.A.). A.S. was supported by a fellowship from the Spanish Ministerio de Educacion, Cultura y Deporte.

Received: August 20, 2003
Revised: January 16, 2004
Accepted: February 10, 2004
Published: April 20, 2004

References

Adair, B.D., and Yeager, M. (2002). Three-dimensional model of the human platelet integrin αIIbβ3 based on electron cryomicroscopy and x-ray crystallography. Proc. Natl. Acad. Sci. USA *99*, 14059–14064.

Alon, R., Kassner, P.D., Carr, M.W., Finger, E.B., Hemler, M.E., and Springer, T.A. (1995). The integrin VLA-4 supports tethering and rolling in flow on VCAM-1. J. Cell Biol. *128*, 1243–1253.

Alonso, J.L., Essafi, M., Xiong, J.P., Stehle, T., and Arnaout, M.A. (2002). Does the integrin αA domain act as a ligand for its βA domain? Curr. Biol. *12*, R340–R342.

Bednar, R.A., Gaul, S.L., Hamill, T.G., Egbertson, M.S., Shafer, J.A., Hartman, G.D., Gould, R.J., and Bednar, B. (1998). Identification of low molecular weight GP IIb/IIIa antagonists that bind preferentially to activated platelets. J. Pharmacol. Exp. Ther. *285*, 1317–1326.

Beglova, N., Blacklow, S.C., Takagi, J., and Springer, T.A. (2002). Cysteine-rich module structure reveals a fulcrum for integrin rearrangement upon activation. Nat. Struct. Biol. *9*, 282–287.

Berlin, C., Bargatze, R.F., von Andrian, U.H., Szabo, M.C., Hasslen, S.R., Nelson, R.D., Berg, E.L., Erlandsen, S.L., and Butcher, E.C. (1995). α4 integrins mediate lymphocyte attachment and rolling under physiologic flow. Cell *80*, 413–422.

Campbell, J.J., Hedrick, J., Zlotnik, A., Siani, M.A., Thompson, D.A., and Butcher, E.C. (1998). Chemokines and the arrest of lymphoyctes rolling under flow conditions. Science *279*, 381–384.

Chen, J.F., Salas, A., and Springer, T.A. (2003). Bistable regulation of integrin adhesiveness by a bipolar metal ion cluster. Nat. Struct. Biol. *10*, 995–1001.

de Chateau, M., Chen, S., Salas, A., and Springer, T.A. (2001). Kinetic and mechanical basis of rolling through an integrin and novel Ca^{2+}-dependent rolling and Mg^{2+}-dependent firm adhesion modalities for the α4β7-MAdCAM-1 interaction. Biochemistry *40*, 13972–13979.

Diacovo, T.G., Catalina, M.D., Siegelman, M.H., and von Andrian, U.H. (1998). Circulating activated platelets reconstitute lymphocyte homing and immunity in L-selectin-deficient mice. J. Exp. Med. *187*, 197–204.

Dransfield, I., and Hogg, N. (1989). Regulated expression of Mg2+ binding epitope on leukocyte integrin alpha subunits. EMBO J. *8*, 3759–3765.

Forlow, S.B., and Ley, K. (2001). Selectin-independent leukocyte rolling and adhesion in mice deficient in E-, P-, and L-selectin and ICAM-1. Am. J. Physiol. Heart Circ. Physiol. *280*, H634–H641.

Forlow, S.B., White, E.J., Barlow, S.C., Feldman, S.H., Lu, H., Bagby, G.J., Beaudet, A.L., Bullard, D.C., and Ley, K. (2000). Severe inflammatory defect and reduced viability in CD18 and E-selectin double-mutant mice. J. Clin. Invest. *106*, 1457–1466.

Fotouhi, N., Gillespie, P., Guthrie, R., Pietranico-Cole, S., and Yun, W. (1999). Month year. Diaminopropionic acid derivatives. Patent Cooperation Treaty International Application number WO0021920.

Gadek, T.R., Burdick, D.J., McDowell, R.S., Stanley, M.S., Marsters, J.C., Jr., Paris, K.J., Oare, D.A., Reynolds, M.E., Ladner, C., Zioncheck, K.A., et al. (2002). Generation of an LFA-1 antagonist by the transfer of the ICAM-1 immunoregulatory epitope to a small molecule. Science *295*, 1086–1089.

Gordon, K.B., Papp, K.A., Hamilton, T.K., Walicke, P.A., Dummer, W., Li, N., Bresnahan, B.W., and Menter, A. (2003). Efalizumab for patients with moderate to severe plaque psoriasis: a randomized controlled trial. JAMA *290*, 3073–3080.

Henderson, R.B., Lim, L.H., Tessier, P.A., Gavins, F.N., Mathies, M., Perretti, M., and Hogg, N. (2001). The use of lymphocyte function-associated antigen (LFA)-1-deficient mice to determine the role of LFA-1, Mac-1, and α4 integrin in the inflammatory response of neutrophils. J. Exp. Med. *194*, 219–226.

Huang, C., and Springer, T.A. (1997). Folding of the β-propeller domain of the integrin α_L subunit is independent of the I domain and dependent on the β_2 subunit. Proc. Natl. Acad. Sci. USA *94*, 3162–3167.

Humphries, M.J. (2000). Integrin structure. Biochem. Soc. Trans. *28*, 311–339.

Huth, J.R., Olejniczak, E.T., Mendoza, R., Liang, H., Harris, E.A., Lupher, M.L., Jr., Wilson, A.E., Fesik, S.W., and Staunton, D.E. (2000). NMR and mutagenesis evidence for an I domain allosteric site that regulates lymphocyte function-associated antigen 1 ligand binding. Proc. Natl. Acad. Sci. USA *97*, 5231–5236.

Jung, U., Norman, K.E., Scharffetter-Kochanek, K., Beaudet, A.L., and Ley, K. (1998). Transit time of leukocytes rolling through venules controls cytokine-induced inflammatory cell recruitment in vivo. J. Clin. Invest. *102*, 1526–1533.

Kallen, J., Welzenbach, K., Ramage, P., Geyl, D., Kriwacki, R., Legge, G., Cottens, S., Weitz-Schmidt, G., and Hommel, U. (1999). Structural basis for LFA-1 inhibition upon lovastatin binding to the CD11a I-domain. J. Mol. Biol. *292*, 1–9.

Knorr, R., and Dustin, M.L. (1997). The lymphocyte function-associated antigen 1 I domain is a transient binding module for intercellular adhesion molecule (ICAM)-1 and ICAM-1 in hydrodynamic flow. J. Exp. Med. *186*, 719–730.

Kouns, W.C., Kirchhofer, D., Hadvary, P., Edenhofer, A., Weller, T., Pfenninger, G., Baumgartner, H.R., Jennings, L.K., and Steiner, B. (1992). Reversible conformational changes induced in glycoprotein IIb-IIIa by a potent and selective peptidomimetic inhibitor. Blood *80*, 2539–2547.

Last-Barney, K., Davidson, W., Cardozo, M., Frye, L.L., Grygon, C.A., Hopkins, J.L., Jeanfavre, D.D., Pav, S., Qian, C., Stevenson, J.M., et al. (2001). Binding site elucidation of hydantoin-based antagonists of LFA-1 using multidisciplinary technologies: evidence for the allosteric inhibition of a protein-protein interaction. J. Am. Chem. Soc. *123*, 5643–5650.

Lawrence, M.B., and Springer, T.A. (1991). Leukocytes roll on a selectin at physiologic flow rates: distinction from and prerequisite for adhesion through integrins. Cell *65*, 859–873.

Lawrence, M.B., Berg, E.L., Butcher, E.C., and Springer, T.A. (1995). Rolling of lymphocytes and neutrophils on peripheral node addressin and subsequent arrest on ICAM-1 in shear flow. Eur. J. Immunol. *25*, 1025–1031.

Liu, G., Huth, J.R., Olejniczak, E.T., Mendoza, R., DeVries, P., Leitza, S., Reilly, E.B., Okasinski, G.F., Fesik, S.W., and von Geldern, T.W. (2001). Novel p-arylthio cinnamides as antagonists of leukocyte function- associated antigen-1/intracellular adhesion molecule-1 interaction. 2. Mechanism of inhibition and structure-based improvement of pharmaceutical properties. J. Med. Chem. *44*, 1202–1210.

Lu, C., and Springer, T.A. (1997). The α subunit cytoplasmic domain regulates the assembly and adhesiveness of integrin lymphocyte function-associated antigen-1 (LFA-1). J. Immunol. *159*, 268–278.

Lu, C., Ferzly, M., Takagi, J., and Springer, T.A. (2001a). Epitope mapping of antibodies to the C-terminal region of the integrin β2 subunit reveals regions that become exposed upon receptor activation. J. Immunol. *166*, 5629–5637.

Lu, C., Shimaoka, M., Ferzly, M., Oxvig, C., Takagi, J., and Springer,

T.A. (2001b). An isolated, surface-expressed I domain of the integrin αLβ2 is sufficient for strong adhesive function when locked in the open conformation with a disulfide. Proc. Natl. Acad. Sci. USA *98*, 2387–2392.

Lu, C., Shimaoka, M., Zang, Q., Takagi, J., and Springer, T.A. (2001c). Locking in alternate conformations of the integrin αLβ2 I domain with disulfide bonds reveals functional relationships among integrin domains. Proc. Natl. Acad. Sci. USA *98*, 2393–2398.

Luo, B.-H., Springer, T.A., and Takagi, J. (2003a). High affinity ligand binding by integrins does not involve head separation. J. Biol. Chem. *278*, 17185–17189.

Luo, B.-H., Springer, T.A., and Takagi, J. (2003b). Stabilizing the open conformation of the integrin headpiece with a glycan wedge increases affinity for ligand. Proc. Natl. Acad. Sci. USA *100*, 2403–2408.

Martin, S., Casasnovas, J.M., Staunton, D.E., and Springer, T.A. (1993). Efficient neutralization and disruption of rhinovirus by chimeric ICAM-1/immunoglobulin molecules. J. Virol. *67*, 3561–3568.

Mould, A.P., Barton, S.J., Askari, J.A., McEwan, P.A., Buckley, P.A., Craig, S.E., and Humphries, M.J. (2003a). Conformational changes in the integrin βA domain provide a mechanism for signal transduction via hybrid domain movement. J. Biol. Chem. *278*, 17028–17035.

Mould, A.P., Symonds, E.J., Buckley, P.A., Grossmann, J.G., McEwan, P.A., Barton, S.J., Askari, J.A., Craig, S.E., Bella, J., and Humphries, M.J. (2003b). Structure of an integrin-ligand complex deduced from solution x-ray scattering and site-directed mutagenesis. J. Biol. Chem. *278*, 39993–39999.

Perry, M.A., and Granger, D.N. (1991). Role of CD11/CD18 in shear rate-dependent leukocyte-endothelial cell interactions in cat mesenteric venules. J. Clin. Invest. *87*, 1798–1804.

Robinson, M.K., Andrew, D., Rosen, H., Brown, D., Ortlepp, S., Stephens, P., and Butcher, E.C. (1992). Antibody against the Leu-cam β-chain (CD18) promotes both LFA-1-and CR3-dependent adhesion events. J. Immunol. *148*, 1080–1085.

Salas, A., Shimaoka, M., Chen, S., Carman, C.V., and Springer, T.A. (2002). Transition from rolling to firm adhesion is regulated by the conformation of the I domain of the integrin LFA-1. J Bio Chem *277*, 50255–50262.

Sanchez-Madrid, F., Krensky, A.M., Ware, C.F., Robbins, E., Strominger, J.L., Burakoff, S.J., and Springer, T.A. (1982). Three distinct antigens associated with human T lymphocyte-mediated cytolysis: LFA-1, LFA-2, and LFA-3. Proc. Natl. Acad. Sci. USA *79*, 7489–7493.

Shimaoka, M., Lu, C., Palframan, R., von Andrian, U.H., Takagi, J., and Springer, T.A. (2001). Reversibly locking a protein fold in an active conformation with a disulfide bond: integrin αL I domains with high affinity and antagonist activity in vivo. Proc. Natl. Acad. Sci. USA *98*, 6009–6014.

Shimaoka, M., Takagi, J., and Springer, T.A. (2002). Conformational regulation of integrin structure and function. Annu. Rev. Biophys. Biomol. Struct. *31*, 485–516.

Shimaoka, M., Salas, A., Yang, W., Weitz-Schmidt, G., and Springer, T.A. (2003a). Small molecule integrin antagonists that bind to the β2 subunit I-like domain and activate signals in one direction and block them in another. Immunity *19*, 391–402.

Shimaoka, M., Xiao, T., Liu, J.-H., Yang, Y., Dong, Y., Jun, C.-D., McCormack, A., Zhang, R., Joachimiak, A., Takagi, J., et al. (2003b). Structures of the αL I domain and its complex with ICAM-1 reveal a shape-shifting pathway for integrin regulation. Cell *112*, 99–111.

Sigal, A., Bleijs, D.A., Grabovsky, V., van Vliet, S.J., Dwir, O., Figdor, C.G., van Kooyk, Y., and Alon, R. (2000). The LFA-1 integrin supports rolling adhesions on ICAM-1 under physiological shear flow in a permissive cellular environment. J. Immunol. *165*, 442–452.

Springer, T.A. (1994). Traffic signals for lymphocyte recirculation and leukocyte emigration: the multi-step paradigm. Cell *76*, 301–314.

Springer, T.A. (2002). Predicted and experimental structures of integrins and β-propellers. Curr. Opin. Struct. Biol. *12*, 802–813.

Stein, J.V., Cheng, G., Stockton, B.M., Fors, B.P., Butcher, E.C., and von Andrian, U.H. (1999). L-selectin-mediated leukocyte adhesion in vivo: Microvillous distribution determines tethering efficiency, but not rolling velocity. J. Exp. Med. *189*, 37–50.

Takagi, J., Petre, B.M., Walz, T., and Springer, T.A. (2002). Global conformational rearrangements in integrin extracellular domains in outside-in and inside-out signaling. Cell *110*, 599–611.

Takagi, J., Strokovich, K., Springer, T.A., and Walz, T. (2003). Structure of integrin α5β1 in complex with fibronectin. EMBO J. *22*, 4607–4615.

Ulmer, A.J., and Flad, H.D. (1979). Discontinuous density gradient separation of human mononuclear leucocytes using Percoll as gradient medium. J. Immunol. Methods *30*, 1–10.

von Andrian, U.H. (1996). Intravital microscopy of the peripheral lymph node microcirculation in mice. Microcirc *3*, 287–300.

von Andrian, U.H., Chambers, J.D., McEvoy, L.M., Bargatze, R.F., Arfors, K.E., and Butcher, E.C. (1991). Two-step model of leukocyte-endothelial cell interaction in inflammation: Distinct roles for LECAM-1 and the leukocyte β_2 integrins *in vivo*. Proc. Natl. Acad. Sci. USA *88*, 7538–7542.

von Andrian, U.H., and M'Rini, C. (1998). In situ analysis of lymphocyte migration to lymph nodes. Cell Adhes Commun *6*, 85–96.

von Andrian, U.H., and Mackay, C.R. (2000). T-cell function and migration. Two sides of the same coin. N. Engl. J. Med. *343*, 1020–1034.

Warnock, R.A., Askari, S., Butcher, E.C., and von Andrian, U.H. (1998). Molecular mechanisms of lymphocyte homing to peripheral lymph nodes. J. Exp. Med. *187*, 205–216.

Weber, C., and Springer, T.A. (1997). Neutrophil accumulation on activated, surface-adherent platelets in flow is mediated by interaction of Mac-1 with fibrinogen bound to αIIbβ3 and stimulated by platelet-activating factor. J. Clin. Invest. *100*, 2085–2093.

Weitz-Schmidt, G., Welzenbach, K., Brinkmann, V., Kamata, T., Kallen, J., Bruns, C., Cottens, S., Takada, Y., and Hommel, U. (2001). Statins selectively inhibit leukocyte function antigen-1 by binding to a novel regulatory integrin site. Nat. Med. *7*, 687–692.

Welzenbach, K., Hommel, U., and Weitz-Schmidt, G. (2002). Small molecule inhibitors induce conformational changes in the I domain and the I-like domain of lymphocyte function-associated antigen-1: molecular insights into integrin inhibition. J. Biol. Chem. *277*, 10590–10598.

Weninger, W., Ulfman, L.H., Cheng, G., Souchkova, N., Quackenbush, E.J., Lowe, J.B., and von Andrian, U.H. (2000). Specialized contributions by alpha(1,3)-fucosyltransferase-IV and FucT-VII during leukocyte rolling in dermal microvessels. Immunity *12*, 665–676.

Woska, J.R., Jr., Shih, D., Taqueti, V.R., Hogg, N., Kelly, T.A., and Kishimoto, T.K. (2001). A small-molecule antagonist of LFA-1 blocks a conformational change important for LFA-1 function. J. Leukoc. Biol. *70*, 329–334.

Xiong, J.-P., Stehle, T., Diefenbach, B., Zhang, R., Dunker, R., Scott, D.L., Joachimiak, A., Goodman, S.L., and Arnaout, M.A. (2001). Crystal structure of the extracellular segment of integrin αVβ3. Science *294*, 339–345.

Xiong, J.P., Stehle, T., Zhang, R., Joachimiak, A., Frech, M., Goodman, S.L., and Arnaout, M.A. (2002). Crystal structure of the extracellular segment of integrin αVβ3 in complex with an Arg-Gly-Asp ligand. Science *296*, 151–155.

Yahalom, D., Wittelsberger, A., Mierke, D.F., Rosenblatt, M., Alexander, J.M., and Chorev, M. (2002). Identification of the principal binding site for RGD-containing ligands in the αVβ3 integrin: a photoaffinity cross-linking study. Biochemistry *41*, 8321–8331.

Yang, W., Shimaoka, M., Chen, J.F., and Springer, T.A. (2004a). Activation of integrin β subunit I-like domains by one-turn C-terminal α-helix deletions. Proc. Natl. Acad. Sci. USA *101*, 2333–2338.

Yang, W., Shimaoka, M., Salas, A., Takagi, J., and Springer, T.A. (2004b). Inter-subunit signal transmission in integrins by a receptor-like interaction with a pull spring. Proc. Natl. Acad. Sci. USA *101*, 2906–2911.

Zang, Q., and Springer, T.A. (2001). Amino acid residues in the PSI domain and cysteine-rich repeats of the integrin β2 subunit that restrain activation of the integrin αXβ2. J. Biol. Chem. *276*, 6922–6929.